
ACTIVE TEACHER SELECTION FOR REINFORCEMENT LEARNING FROM HUMAN FEEDBACK

A PREPRINT

Rachel Freedman*
EECS
UC Berkeley
rachel.freedman@berkeley.edu

Justin Svegliato
EECS
UC Berkeley
jsvegliato@berkeley.edu

Kyle Wray
Computer Science
Stanford
kylewray@stanford.edu

Stuart Russell
EECS
UC Berkeley
russell@berkeley.edu

October 25, 2023

ABSTRACT

Reinforcement learning from human feedback (RLHF) enables machine learning systems to learn objectives from human feedback. A core limitation of these systems is their assumption that all feedback comes from a single human teacher, despite querying a range of distinct teachers. We propose the *Hidden Utility Bandit* (HUB) framework to model differences in teacher rationality, expertise, and costliness, formalizing the problem of learning from multiple teachers. We develop a variety of solution algorithms and apply them to two real-world domains: paper recommendation systems and COVID-19 vaccine testing. We find that the *Active Teacher Selection* (ATS) algorithm outperforms baseline algorithms by actively selecting when and which teacher to query. The HUB framework and ATS algorithm demonstrate the importance of leveraging differences between teachers to learn accurate reward models, facilitating future research on active teacher selection for robust reward modeling.

1 Introduction

Specifying objective functions for machine learning systems is challenging, and misspecified objectives can be hacked [1, 2] or incentivise degenerate behavior [3, 4, 5]. Techniques such as *reinforcement learning from human feedback* (RLHF) enable ML systems to instead *learn* appropriate objectives from human feedback [6, 7, 8]. These techniques are widely used to finetune large language models [9, 10, 11, 12] and to train reinforcement learning agents to perform complex maneuvers in continuous control environments [6, 7]. However, while RLHF is relied upon to ensure that these systems are safe, helpful, and harmless [13], it still faces many limitations and unsolved challenges [14].

In particular, RLHF systems typically rely on the assumption that all feedback comes from a single human teacher, despite gathering feedback from a range of teachers with varying levels of rationality and expertise. For example, Stiennon et al. [8], Bai et al. [13] and Ouyang et al. [15] assume that all feedback comes from a single teacher, but find that annotators and researchers actually disagree 23% to 37% of the time. Reward learning has been shown to be highly sensitive to incorrect assumptions about the process that generates feedback [16, 17, 18, 19], so this single-teacher assumption exposes these systems to dangerous failures [20]. Ideally, RLHF systems should consider the differences between each teacher to improve their safety and reliability.

To leverage multiple teachers in RLHF, we introduce a novel problem called a *Hidden Utility Bandit* (HUB), illustrated in Figure 1. In a HUB, the learning agent must choose between pulling an arm to earn utility (as in a standard

*corresponding author

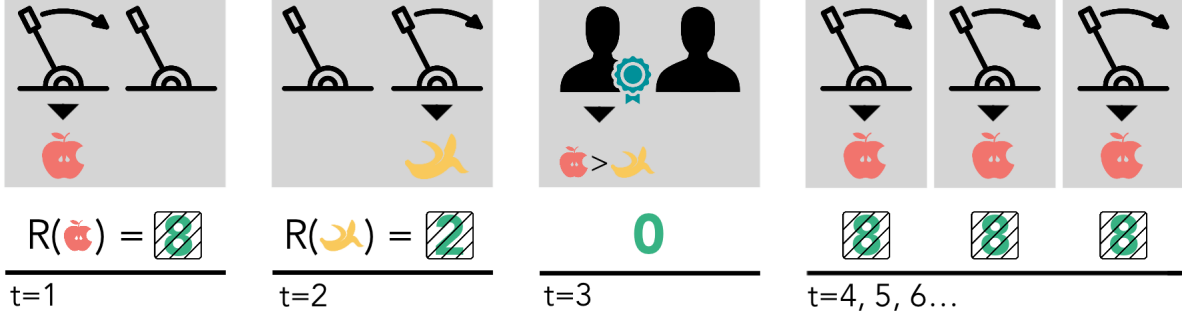


Figure 1: A simple *Hidden Utility Bandit (HUB)* with two arms and two teachers. The agent pulls the first arm, observes an apple, and receives the apple’s utility of 8 without observing it. The agent then pulls the second arm, observes a banana, and receives the banana’s utility of 2 without observing it. Because these utilities are hidden, the agent foregoes the opportunity for utility on the third timestep to ask the expert teacher which fruit is better. The expert replies that apples are better than bananas, so the agent pulls the first arm to maximize apples for all remaining timesteps.

multi-armed bandit) and querying a teacher for feedback to learn the utility function (as in RLHF). Optimal HUB solutions must therefore actively select *which* teachers to query *when* so as to maximize the expected discounted sum of utilities.

In this paper, we begin by formalizing the HUB framework and proposing a naive baseline solution (Section 2). We then develop an *Active Teacher Selection (ATS)* method that selects *which* teachers to query *when* to maximize cumulative discounted utility (Section 3). Since there are no existing solutions to the novel HUB problem, we introduce multiple families of baseline methods and evaluate these against ATS variations on a realistic paper recommendation task (Section 4.1). ATS outperforms methods with fixed exploration windows, demonstrating the usefulness of selecting *when* to query teachers, and ATS with specific teacher selection outperforms general teacher selection, underscoring the usefulness of selecting *which* teacher to query. As a proof-of-concept, we also demonstrate how this framework can be applied to the real-world problem of evaluating COVID-19 vaccines with noisy tests (Section 4.2). The result is a HUB framework and an ATS algorithm² that demonstrate the importance of leveraging differences between teachers to learn accurate reward models. These will facilitate and benchmark improved methods, ultimately leading to scalable reward learning algorithms that learn accurate, robust and value-aligned models.

2 Hidden Utility Bandits

We design the *Hidden Utility Bandit (HUB)* framework to formalize the problem of reward learning from multiple teachers. Formally, a HUB is a stochastic multi-armed bandit problem where the utilities received from pulling arms are hidden from the agent solving the problem. To learn these utilities, the agent asks for feedback from human teachers who directly observe them but only provide noisy feedback. Following an existing standard in work on RLHF [7], a HUB models each teacher as Boltzmann-rational with its noisiness modulated by a *rationality parameter* $\beta \in [0, \infty)$. In particular, the probability that a teacher with rationality parameter β prefers item i to j is below:

$$\Pr(i \succ j; \beta, \mathcal{U}) = \frac{\exp(\beta \mathcal{U}(i))}{\exp(\beta \mathcal{U}(i)) + \exp(\beta \mathcal{U}(j))}, \quad (1)$$

where $\mathcal{U} : \mathcal{I} \rightarrow \mathbb{R}$ gives the true utility of all items in set \mathcal{I} .

At each timestep of the HUB problem, the agent chooses between pulling a bandit arm, receiving a hidden utility sampled from that arm’s distribution, or querying a teacher, receiving feedback modulated by that teacher’s rationality parameter but incurring that teacher’s query cost. Its objective is to maximize the expected discounted sum of utilities, so it must balance querying costly teachers to learn about the utility function with pulling arms to earn utility. We turn to a formal description of the HUB problem below.

Definition 2.1. A *hidden-utility bandit (HUB)* is a tuple $\langle \mathcal{I}, \mathcal{U}, \mathcal{C}, \beta, F, Q, \gamma \rangle$:

- \mathcal{I} is a set of N items, each associated with a hidden utility.
- $\mathcal{U} : \mathcal{I} \rightarrow [u_{min}, u_{max}]$ is a *utility function* over \mathcal{I} , where \mathbb{U} is the utility function space.

²Our open-source ATS Julia library is available at [github.com/\[redacted\]/ATS](https://github.com/[redacted]/ATS).

- $\mathcal{C} = \{c^1, c^2, \dots, c^K\}$ is a set of K arm choices, each associated with an arm distribution $\mathcal{D}^k : \mathcal{I} \rightarrow [0, 1]$ giving the probability of returning each item in \mathcal{I} , where $\mathbb{D} = \mathbb{D}^1 \times \mathbb{D}^2 \times \dots \times \mathbb{D}^K$ is the joint arm distribution space over all arm choices \mathcal{C} .
- $\beta = \{\beta^1, \beta^2, \dots, \beta^M\}$ is a set of M teacher rationality parameters.
- $F = \{f^1, f^2, \dots, f^M\}$ is a set of M teacher query costs.
- $Q : \mathcal{I} \times \mathcal{I} \rightarrow [0, 1]$ is a query profile that gives probabilities of picking queries in $\binom{\mathcal{I}}{2}$.
- γ is a discount factor.

Here, the agent can observe \mathcal{I} , \mathcal{C} , β , F , Q , and γ but cannot observe the utility function \mathcal{U} or the arm distributions \mathcal{D} . At each timestep t , the agent can select an arm choice $c_t \in \mathcal{C}$ or a teacher rationality parameter $\beta_t \in \beta$. If the agent pulls an arm choice $c_t \in \mathcal{C}$, it observes an item i_t sampled from the arm distribution \mathcal{D}^{c_t} and receives but does *not* observe the utility $u_t = \mathcal{U}(i_t)$. Conversely, if the agent queries a teacher with rationality parameter $\beta_t \in \beta$, it receives and observes an item pair (i, j) sampled from the query profile Q , a preference p_t sampled from $\text{Bernoulli}(P)$ given the probability $P = \Pr(i \succ j; \beta_t, \mathcal{U})$ in Equation 1, and the teacher query cost $u_t = f^{\beta_t}$.

Since the agent’s objective is to maximize the expected discounted sum of utilities $\mathbb{E}[\sum_{t=0}^{\infty} \gamma^t u_t]$, it must balance querying teachers to learn about the utility function with selecting bandit arms to earn utility. Standard RLHF systems alternate between fitting a reward model to teacher feedback and learning a policy using the reward model on a predefined schedule. However, the HUB framework allows the agent to interweave these processes to optimize performance.

2.1 Naive HUB Inference

We propose a naive HUB inference baseline in Algorithm 1. This allows the agent to infer the hidden information: the joint arm distribution $\mathcal{D}^{\mathcal{C}} = (\mathcal{D}^1, \mathcal{D}^2, \dots, \mathcal{D}^K)$ (common to stochastic multi-armed bandit problems) and utility function \mathcal{U} (unique to the HUB).

In Algorithm 1, the agent randomly pulls arms and queries a preselected teacher for a fixed number of timesteps and then uses sample means to approximate the true joint arm distribution and true teacher preference probabilities. Using these approximate teacher preference probabilities, the *difference* in utility values for items i and j , $\Delta_{ij} = \mathcal{U}(i) - \mathcal{U}(j)$, can be calculated in the following way:

$$\Pr(i \succ j; \beta^m, \mathcal{U}) = \frac{1}{1 + \exp(-\beta^m \Delta_{ij})} \implies \Delta_{ij} = -\frac{1}{\beta^m} \ln \left[\frac{1}{\Pr(i \succ j; \beta^m, \mathcal{U})} - 1 \right]. \quad (2)$$

Thereafter, the utility values of individual items i and j can be calculated from these differences Δ_{ij} using the maximum and minimum values of \mathcal{U} . After deriving these estimates, the agent simply selects the arm with the highest expected utility for the remainder of the episode.

Despite the simplicity of Algorithm 1, it is possible to prove that it converges to the true \mathcal{U}^* and $\mathcal{D}^{\mathcal{C}*}$ in the limit of infinite queries. We prove the following theorem in Appendix A:

Theorem 1. *If the predicted utility function $\hat{\mathcal{U}}$ and the predicted arm distribution $\hat{\mathcal{D}}^{\mathcal{C}}$ are estimated by executing Algorithm 1 with T samples, then $\hat{\mathcal{U}} \rightarrow \mathcal{U}^*$ and $\hat{\mathcal{D}}^{\mathcal{C}} \rightarrow \mathcal{D}^{\mathcal{C}*}$ as $T \rightarrow \infty$.*

However, exploring randomly for a fixed number of timesteps and querying a fixed teacher may be suboptimal. By maintaining and updating an internal belief over the hidden information, the agent can query teachers only when teacher feedback is necessary to update its belief.

3 Active Teacher Selection

The *Active Teacher Selection (ATS)* algorithm solves the HUB problem efficiently by maintaining a belief over the utility function and arm distributions, and choosing when to query teachers. This allows it to only query teachers when required for decision-relevant belief updates. ATS can also actively select *which* teacher to query. When teachers are “noisy” ($\beta < \infty$), the preference probability $\Pr(i \succ j; \beta, \mathcal{U})$ correlates with the difference in utility between i and j , so it will sometimes be more informative for ATS to select teachers with *lower* β values [21, 22]. Importantly, this removes the need to set the problem-specific hyperparameters in Algorithm 1 for exploration (T) and teacher selection (β^m).

Algorithm 1 NAIVEHUBINFERENCE(\cdot)**Require:** HUB $\langle \mathcal{I}, \mathcal{U}, \mathcal{C}, \beta, F, Q, \gamma \rangle, u_{\min}, u_{\max}, T$ samples, β^m of selected teacher**Initialize:** $frequency[c], frequency[c][i], frequency[b][q], preferences[b][q]$

```

1: for  $t = 1, \dots, T$  do
2:   if sampleUniformly({TRUE, FALSE}) then
3:     sample  $c \sim \mathcal{C}$  ▷ Sample arm uniformly at random
4:     sample  $i \sim \mathcal{D}^c$  ▷ Sample item from (unobserved) arm distribution
5:      $frequency[c] \leftarrow frequency[c] + 1$ 
6:      $frequency[c][i] \leftarrow frequency[c][i] + 1$ 
7:   else
8:     sample  $b \sim \beta$  ▷ Sample teacher uniformly at random
9:     sample  $q = (i, j) \sim Q$  ▷ Sample query from query profile
10:    sample  $p \sim \text{Bernoulli}(\text{Pr}(i \succ_j; b, \mathcal{U}))$  ▷ Sample preference given Equation 1
11:     $frequency[b][q] \leftarrow frequency[b][q] + 1$ 
12:     $preferences[b][q] \leftarrow preferences[b][q] + p$ 
13:   $\hat{D}^c(i) \leftarrow \frac{frequency[c][i]}{frequency[c]} \quad \forall c \in \mathcal{C}, i \in \mathcal{I}$  ▷ Estimate arm distributions
14:   $\hat{P}(b, q) \leftarrow \frac{preferences[b][q]}{frequency[b][q]} \quad \forall b \in \beta, q \in Q$  ▷ Estimate preference probabilities
15:   $\Delta_{ij} = -\frac{1}{\beta^m} \ln \left[ \frac{1}{\hat{P}(\beta^m, q=(i,j))} - 1 \right] \quad \forall i, j \in \mathcal{I}$  ▷ Calculate using Equation 2
16:   $(x, y) \leftarrow \operatorname{argmax}_{x,y} [\Delta_{xy}]$  ▷ Find indices of maximum element
17:   $\hat{\mathcal{U}}(y) \leftarrow u_{\min}, \quad \hat{\mathcal{U}}(i) \leftarrow \left[ \frac{u_{\max}}{u_{\max} - u_{\min}} \right] \Delta_{iy} + u_{\min} \quad \forall i \in \mathcal{I} \setminus \{y\}$  ▷ Estimate utilities

```

3.1 ATS Algorithm

The ATS algorithm has two general steps: the HUB is first converted to a simplified partially observable Markov decision process (POMDP) [23] and then solved using a Monte Carlo POMDP solver with custom rollout policies.

Constructing the HUB-POMDP The HUB-POMDP state contains the HUB utility function and arm distributions. Since these are fixed for a given HUB, the state does not change over time, making the HUB-POMDP simpler than a traditional POMDP. The HUB-POMDP reward function gives the *expected* utility of each arm according to this state.

Definition 3.1. A **hidden utility bandit POMDP (HUB-POMDP)** is a tuple $\langle \mathcal{S}, \mathcal{A}, \mathcal{T}, \mathcal{R}, \Omega, \mathcal{O} \rangle$:

- $\mathcal{S} = \mathbb{U} \times \mathbb{D}$ is the state space: the state $s \in \mathcal{S}$ is a tuple $\langle \mathcal{U}, \mathcal{D}^c \rangle$ that is fixed.
- $\mathcal{A} = \mathcal{C} \cup \beta$ is the action space: the arm choices \mathcal{C} and teachers β .
- $\mathcal{T} : \mathcal{S} \times \mathcal{A} \rightarrow \mathcal{S}$ is the stationary transition function: $\mathcal{T}(s, a) = s \quad \forall s \in \mathcal{S} \quad \forall a \in \mathcal{A}$.
- $\mathcal{R} : \mathcal{S} \times \mathcal{A} \rightarrow \mathbb{R}$ is the reward function:

$$\mathcal{R}(s, a) = \begin{cases} \sum_{i \in \mathcal{I}} \mathcal{U}(i) \mathcal{D}^a(i) & \text{if } a \in \mathcal{C} \\ f^a & \text{if } a \in \beta \end{cases}$$

- $\Omega : \mathcal{I} \cup \mathbb{P}$ is the observation space: the items \mathcal{I} and query-preferences $\mathbb{P} = \mathcal{I} \times \mathcal{I} \times \{0, 1\}$.
- $\mathcal{O} : \mathcal{A} \times \Omega \rightarrow [0, 1]$ is the observation function:

$$\mathcal{O}(a, \omega) = \begin{cases} \mathcal{D}^a(i) & \text{if } a \in \mathcal{C} \\ Q(i, j) \text{Pr}(i \succ_j; \beta^m = a, \mathcal{U}) & \text{if } a \in \beta \end{cases}$$

Teacher selection can be *general* or *specific*. Under specific selection, the agent chooses which teacher to query. The HUB-POMDP's action space contains all M teachers, $\mathcal{A} = \mathcal{C} \cup \beta$, as shown in the HUB-POMDP above. Under general selection, the agent chooses *when* to query a teacher, but not *which* teacher to query. The HUB-POMDP's action space is modified to contain a single general teacher selection action, $\mathcal{A} = \mathcal{C} \cup \{\beta^g\}$. These alternatives offer a tradeoff: general selection reduces the state space size, and thus the computational complexity, while specific selection provides the agent with additional control over its feedback. Our experimental results (reported in Section 4.1) indicate that specific greatly outperforms general teacher selection, so we will use ATS with specific teacher selection unless otherwise specified.

Paper Category	Relevance	Professor	Rationality	Cost	Conference	ICLR			ICML			AAAI		
Application	8	Professor 1	0	0	Paper Distribution	A	B	T	A	B	T	A	B	T
Benchmark	5	Professor 2	0.01	0	Expected Relevance	0.8	0	0.2	0.2	0.8	0	0.2	0.2	0.6
Theory	1	Professor 3	50	0		6.6			5.6			3.2		

Figure 2: Paper recommendation as a HUB problem. Paper categories (Application, Benchmark, Theory) are items (\mathcal{I}), professors are teachers with rationality (β) and cost (F) parameters, conferences are arms with distributions (\mathcal{D}), and relevance scores are utilities (\mathcal{U}). The goal is to recommend the most relevant conferences to read papers from.

Solving the POMDP While exact POMDP solutions are typically intractable, approximate POMDP algorithms often perform well. *Partially observable Monte Carlo planning (POMCP)* algorithms produce time-efficient online solvers that form a belief tree of fixed depth and use rollouts to estimate leaf node values [24]. *POMCP with observation widening (POMCPOW)* uses a weighted particle filter to efficiently produce approximate solutions for problems with large state spaces [25]. We describe and compare candidate rollout policies that we designed specifically for the HUB problem in Appendix C. ATS with the custom *best arm* rollout policy performs best, so we use that rollout policy for our experiments.

3.2 Teacher Noise Inference in ATS

RLHF systems typically assume that the teacher rationality parameters β are known. However, if β is unknown, we show in Theorem 2 that it can be estimated from preference data prior to running ATS. Specifically, given $\Pr(i \succ j; \beta_m, \mathcal{U})$, it is possible to analytically calculate $\beta_m \in \beta$ to within a scaling factor a based on the difference $\Delta_{ij} = \mathcal{U}(i) - \mathcal{U}(j)$. The full procedure involves gathering preference data using an exploration policy or real-world data sources, then estimating $\hat{\beta}_m$, calculating $\beta_m = a \cdot \hat{\beta}_m$ if Δ_{ij} is known, and finally running ATS using the result.³ We demonstrate this procedure in our experiments in Section 4.2 and prove the theorem below in Appendix B.

Theorem 2. *Given two items $i, j \in \mathcal{I}$ where $\mathcal{U}(i) < \mathcal{U}(j)$, the preference probability $P = \Pr(i \succ j; \beta_m, \mathcal{U})$ from Equation 1, and the scaling factor $a = -\Delta_{ij}^{-1}$, we can calculate β_m as follows:*

$$\beta_m = a \cdot \ln\left(\frac{1}{P} - 1\right). \tag{3}$$

The scaling factor a is determined by the item pair (i, j) , so if the same item pair is used to evaluate each teacher, all rationality estimates $\hat{\beta}_m$ will be on the same scale. As we show in our experiments, this scaling factor can be computed directly if \mathcal{U} is known. In addition, we evaluate this procedure in simulation by setting $\beta = \{0.01, 1.0\}$, running a random policy for 1000 timesteps, estimating $\{\hat{\beta}_1, \hat{\beta}_2\}$, and scaling the estimate so that the greatest value is equal to 1.0. After 100 simulations, we observe a mean squared error of only 0.061, indicating that this procedure is accurate.

4 Experiments

We apply the HUB framework to two real-world domains: *paper recommendations* and *COVID-19 vaccine testing*. In the recommendation domain, we conduct comprehensive experiments that evaluate the performance of various solution algorithms (Section 4.1), compare rollout simulation policies (Appendix C), and examine the impact of varying teacher query costs (Appendix D). The more complex vaccine domain provides a proof-of-concept, using the HUB framing to address an urgent problem and demonstrating how β values can be estimated from real-world data. We find that the HUB framework captures both problems well, that the ATS algorithm outperforms all baselines in comprehensive testing in the recommendation domain, and that ATS is the best-performing algorithm that also identifies the best vaccine in the vaccine domain proof-of-concept.

Algorithms We fix ATS to use *specific* teacher selection and the *best arm* rollout policy unless otherwise specified. To our knowledge, the HUB problem is novel and has no solutions in prior literature, so we construct multiple families of baseline methods (*naive* and *random*) for comparison. *Naive* algorithms choose randomly amongst pulling arms and querying the selected teacher for T timesteps, use these observations to estimate the arm distributions and utility

³Note that it is also possible to directly add β to the state space of the HUB-POMDP and then solve it, but this increases the size of the state space and makes the problem less tractable.

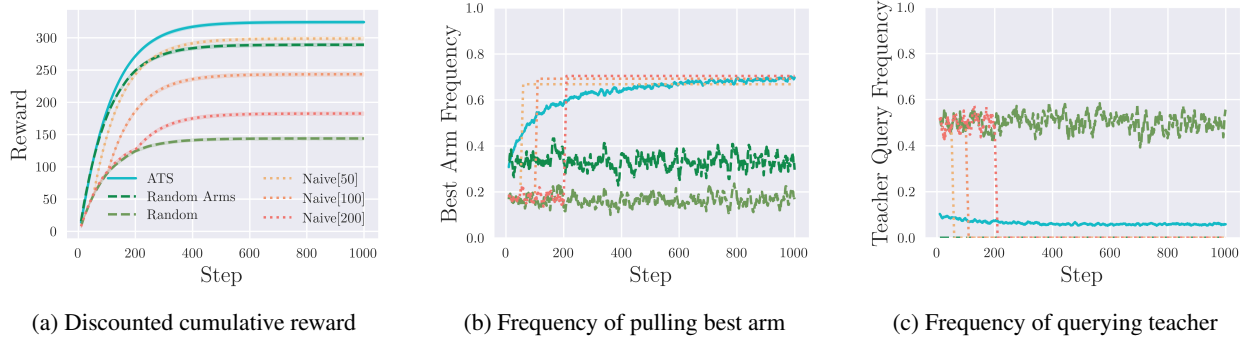


Figure 3: Comparison of ATS, naive and random algorithms. ATS best maximizes discounted reward (a) and identifies the highest-reward arm more often than most baselines and comparably with Naive[100] and Naive[200], which explore more and earn less reward (b). ATS initially queries teachers less often than naive baselines, but continues querying teachers throughout the episode (c). All data is averaged across 25 runs on 20 HUB problems and smoothed over 10 steps.

function (using Algorithm 1), and then pull the arm with the highest estimated expected utility at each subsequent timestep. Naive algorithms require problem-specific hyperparameters β^m and T , so for these experiments we select the intermediate of 3 teachers ($\beta^m = \beta^2$) and test a range of exploration horizons ($T \in [50, 100, 200]$). *Random* algorithms select actions uniformly at random from a given set. We evaluate a random algorithm that selects actions from the entire action space, as well as one that selects only arms.

4.1 Conference Recommendation Domain

In the recommendation domain, the system recommends AI conferences from which to read relevant papers. There are three paper categories (Application, Benchmark, Theory) with specified relevance scores, and three conferences (ICLR, ICML, AAAI) with different paper category compositions⁴. The recommender cannot directly observe the relevance scores, so it must learn them by asking professors, whose judgements vary from completely random ($\beta^1 = 0$) to highly accurate ($\beta^3 = 50$). In these experiments, query costs are always 0. (See Appendix D for experiments varying query costs.) Each day, the system recommends one conference, a paper is sampled from that conference’s distribution, and the system earns a hidden utility score representing that paper’s category’s relevance. Alternatively, the system queries a professor who provides a preference over a pair of paper categories. Applying the HUB framework, paper categories are the item set $\mathcal{I} = \{A, B, T\}$, relevance scores are the hidden utility function \mathcal{U} , conferences are arm choices $\mathcal{C} = \{c^1 = \text{ICLR}, c^2 = \text{ICML}, c^3 = \text{AAAI}\}$, and professors are teachers with rationality $\beta = \{\beta^1 = 0, \beta^2 = 0.01, \beta^3 = 50\}$.

Figure 2 shows an example paper recommendation problem in which it will sometimes be more informative to query the noisy Professor 2 over the more rational Professor 3. This is because the frequency with which a noisy teacher prefers a lower-reward item over a higher-reward one gives information about the difference between the rewards, and in this example the recommender must learn *how much* more relevant Application papers are than Benchmark papers. Without this information, the system cannot distinguish between cases where $\mathcal{U}(A) = 8$ (indicating that the expected relevance of ICLR is greater than ICML) and where $\mathcal{U}(A) = 6$ (indicating the reverse).

Experiments We evaluate all algorithms for 25 runs of 1000 timesteps on 20 different paper recommendation tasks. Each task is a HUB with \mathcal{I} , \mathcal{C} , and β as described above and a unique tuple $\langle \mathcal{U}, \mathcal{D}^c \rangle$. \mathbb{U} and \mathbb{D} are discretized, and each task’s $\langle \mathcal{U}, \mathcal{D}^c \rangle$ is chosen such that c^1 has the highest expected relevance ($\mathbb{E}[\mathcal{U}(i \sim c^1)] > \mathbb{E}[\mathcal{U}(i \sim c^2)] \geq \mathbb{E}[\mathcal{U}(i \sim c^3)]$) and all paper distributions are different and non-deterministic ($\mathcal{D}^j \neq \mathcal{D}^k \forall j, k \in \mathcal{C}$ and $\mathcal{D}^c(i) \neq 1.0 \forall i \in \mathcal{I}, c \in \mathcal{C}$).

Results While all non-random algorithms successfully identify the most relevant conference in expectation (Figure 3b), ATS with specific teacher selection best balances querying teachers with recommending papers, achieving the highest average discounted cumulative reward (Figure 3a), and most accurately learning relevance scores (Figure 4).

Figure 3b shows how often each algorithm learns to pull the best HUB arm and therefore recommend the most relevant conference over the course of training. All HUB solution methods (ATS, Naive[50], Naive[100], Naive[200]) successfully identify the most relevant conference, recommending it about three times as often as they would if

⁴Example relevance scores and paper category compositions were selected arbitrarily.

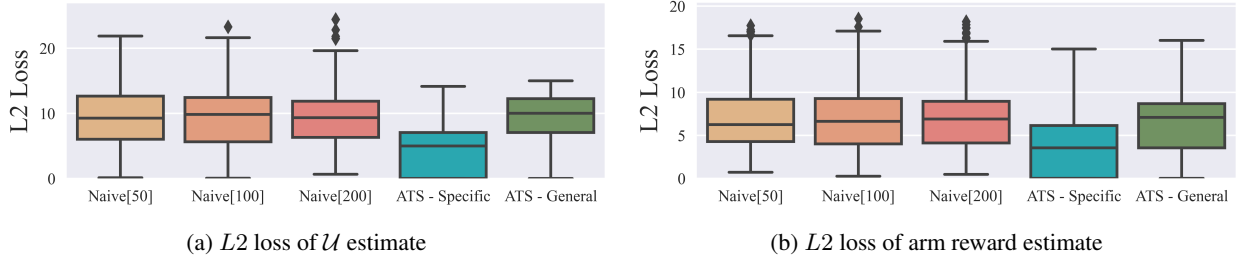


Figure 4: Accuracy of reward learning using ATS (with specific and general teacher selection) and naive algorithms (with exploration parameters of 50, 100, and 200). ATS with specific teacher selection learns both the underlying utility function (a) and the expected rewards of each arm (b) much more accurately than ATS with general teacher selection and naive algorithms. Accuracy is measured as L2 loss, aggregated across 25 runs on 20 HUB problems. The middle line is the median, the boxes are the IQR, the whiskers are 1.5 times the IQR, and the diamonds are outliers.

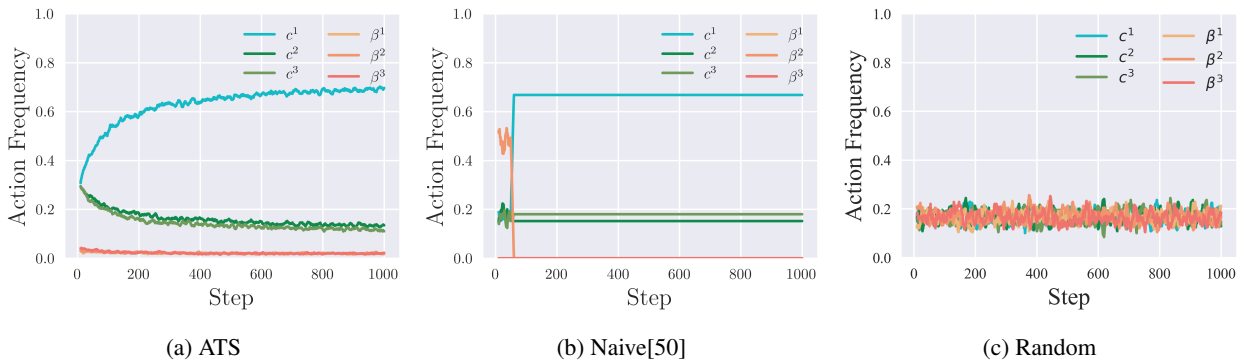


Figure 5: Mean action frequencies for various algorithms. c actions are arm pulls and β actions are teacher queries. Data is averaged across 25 runs of 20 HUB problems and smoothed over 10 steps.

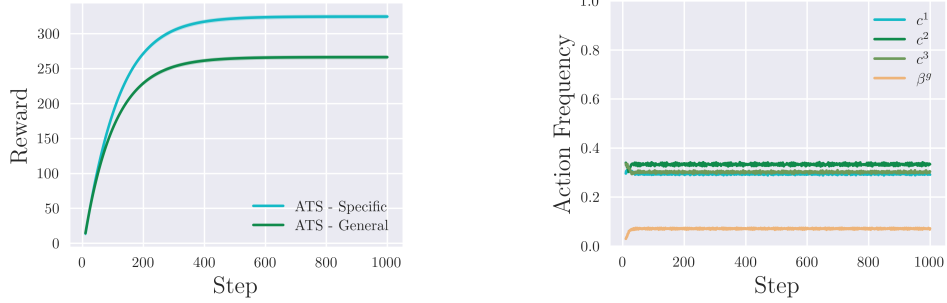
they were behaving randomly (“Random” baseline, light green line) and about twice as often as if they were blindly recommending conferences (“Random Arms” baseline, dark green line). This indicates that the HUB formalism can be used to accurately represent the paper recommendation problem.

While all solution methods identify the best arm, ATS does so most efficiently, querying teachers sparingly even at the start of the task (Figure 3c) and best optimizing the HUB objective of expected discounted cumulative reward (Figure 3a). Moreover, ATS forms the most accurate estimates of the utility function and expected conference relevance scores (Figure 4) after 1000 timesteps, while continuing to explore and potentially improve this estimate by occasionally querying teachers and recommending other conferences (Figure 5a). In contrast, Naive algorithms stop learning after their hand-specified exploration horizon (Figure 5b), and Random algorithms never learn at all (Figure 5c). This demonstrates the benefits of actively selecting when to query teachers, as in ATS, rather than following a predefined schedule, as in standard RLHF.

Figure 6 compares ATS with specific and general teacher selection. Standard RLHF systems do not allow the agent to select which teacher to query and are most akin to general selection. However, we show that the additional control afforded by specific selection allows ATS to make more informative queries. Figure 6a shows that ATS with specific teacher selection earns higher expected reward than ATS with general teacher selection, and Figure 6b shows that ATS with general teacher selection queries all arms roughly equally, failing to identify the one with highest expected reward.

4.2 COVID-19 Vaccine Testing Domain

Bandit problems are commonly used to model medical treatment investigation, so as a proof-of-concept we apply the HUB framework to a real-world medical problem: evaluating vaccines for the 2019 Novel Coronavirus (COVID-19). This task is complicated by the difficulty of evaluating whether a patient is infected: many infections are asymptomatic, and other common illnesses cause similar symptoms. There are a variety of ways to test whether patients have COVID-19, including symptom surveys, antigen tests, and RT-PCR tests, but these vary widely in accuracy and cost.



(a) Specific teacher selection outperforms general teacher selection.

(b) ATS with general teacher selection doesn't identify the best arm.

Figure 6: Performance of ATS with specific and general teacher selection. All data is averaged across 25 runs on 20 HUB problems, smoothed over 10 steps, and discounted with $\gamma = 0.99$.

Symptoms	Utility	Test	Rationality	Cost	Vaccine	Vaccine A			Vaccine B			No Vaccine				
None	8.0	Survey	0.36	-0.006	Symptom Distribution	N	C	F	N	C	F	N	C	F		
Cough	3.0	Antigen	1.32	-0.21		0.9	0.1	0	0.6	0.3	0.1	0.5	0.3	0.2		
Fever	0.5	RT-PCR	2.54	-0.31		Expected Utility			7.5			5.75			5.0	

Figure 7: COVID-19 vaccine testing as a HUB problem. Symptoms (None, Cough, Fever) are items (\mathcal{I}), tests are teachers with rationality (β) and cost (F) parameters, and vaccines are arms (\mathcal{C}) with the specified distributions over patient symptoms (\mathcal{D}).

The HUB framework directly models these challenges. Let the item set be easily observable patient symptoms, $\mathcal{I} = \{\text{None, Cough, Fever}\}$. The ‘‘arms’’ are vaccine candidates, $\mathcal{C} = \{c^1 = \text{VaccineA}, c^2 = \text{VaccineB}, c^3 = \text{NoVaccine}\}$, and the ‘‘teachers’’ are COVID-19 test types, $\{\text{Survey, Antigen, RT-PCR}\}$. Surveys are the least accurate but least expensive, while RT-PCR tests are the most accurate and most expensive. We estimate the US dollar cost of surveys at \$1.20 (accounting for 10 minutes of time at the US federal minimum wage of \$7.25), antigen tests at \$42, and RT-PCR tests at \$62 (median prices reported by [26]), then scale these costs by 0.05. We estimate β by gathering real-world data on the sensitivity of COVID-19 symptom surveys [27], antigen tests [28], and RT-PCR tests [29], interpret this sensitivity as the probability P of the test ‘‘preferring’’ a patient with no COVID-19 ($\mathcal{U} = u_{max}$) to a patient with definite COVID-19 ($\mathcal{U} = u_{min}$), and calculate β_m using Equation 3. We construct arm distributions where patients display the most frequent and severe symptoms with no vaccination, and the least symptoms with Vaccine A, and a utility function where symptoms that have a greater chance of indicating COVID-19 infection have lower scores. These values are reported in Figure 7.

Experiments We evaluate all algorithms for 25 runs of 1000 timesteps on this COVID-19 task. \mathbb{U} and \mathbb{D} are more finely discretized than in the recommendation HUB in order to allow for more realistic values, so the resulting HUB-POMDP has 5 times more states and is more challenging to solve. While the recommendation experiments averaged results over many problem parameters, here we fix the parameters to the values reported in Figure 7, since they are derived from real-world data and realistic estimates.

Results Figure 8 summarises the results. Several algorithms perform well: ATS, Random Arms, and Naive[50] (Figure 8a). The Random Arms baseline that randomly administers vaccines without testing for COVID-19 performs surprisingly well due to the high cost of reliable testing. However, in this domain, we care not only about vaccinating as many people as possible during the trial, but also about identifying which vaccine performs best. ATS clearly identifies the best vaccine, using it increasingly frequently during the trial (Figure 8b). The Naive algorithms also identify the best vaccine, but conduct more costly tests than necessary, leading to poorer overall performance.

5 Related Work

Multi-Armed Bandits *Multi-armed bandits* (MAB) are stateless sequential decision-making problems [30, 31]. At each timestep $h = 1, 2, \dots, H$, the agent chooses one of K arms, each with a distribution over utilities. When the agent

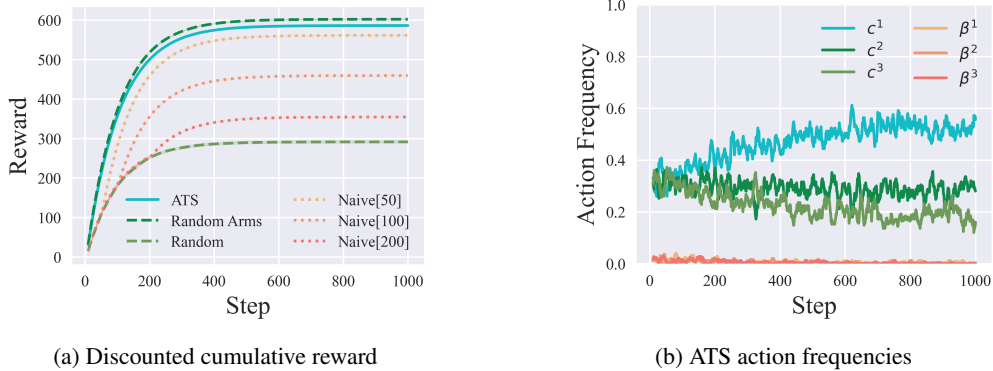


Figure 8: Performance of all algorithms and ATS action frequencies on the COVID-19 vaccine testing problem. Random Arms and ATS both earn high reward from frequently vaccinating participants (a), though only ATS additionally identifies the most effective vaccine (b). Data is averaged across 25 runs and smoothed across 10 steps.

pulls arm $k \in K$, it receives utility sampled from arm k 's distribution $u \sim \mathcal{D}^k$. The agent's goal is to maximize its expected cumulative utility. Our framework is similarly structured, though arm utilities are hidden (as in many real-life applications), and the agent must learn about them from teacher preferences (as in RLHF).

Inverse Reinforcement Learning *Inverse reinforcement learning* (IRL) is a reward learning technique in which the agent infers a reward function given behavioral samples from an optimal policy [32, 33] or a noisy teacher [34]. It is similar to RLHF in that reward information comes from a teacher rather than the environment, but distinct in that it requires teachers to perform the task well themselves [19]. RLHF and the HUB framework are most useful in domains such as those presented in Section 4, where the teacher can distinguish good performance, but does not know how to produce it themselves.

Cooperative Inverse Reinforcement Learning *Cooperative inverse reinforcement learning* (CIRL) extends the IRL framework to allow cooperation and collaboration between the agent and the teacher [35, 36]. HUB problems can be viewed as a specific class of CIRL games in which there are multiple humans, but they can only act (by providing feedback) when the agent requests it (by querying them). However, CIRL problems are DEC-POMDPs, which are NEXP-complete and thus functionally intractable [37]. By fixing the human policy and arm distributions, the HUB framework reduces the problem to a POMDP with a stationary transition function, which is much more tractable. Optimal agent solutions to the CIRL game balance inference and control to produce several qualitatively valuable behaviors, such as only asking the human questions when necessary [38]. The algorithm that best solves the HUB problem, ATS, demonstrates similarly conservative querying behavior.

6 Conclusion

We formalized the teacher selection problem in reward learning and proposed a solution method that expresses this problem as a POMDP. Our empirical results underscore the applicability of this framework to real-world problems, as well as the importance of modeling human teachers as distinct entities and actively choosing *when* and *which* teacher to query.

The purpose of this paper is to investigate the novel problem of selecting teachers in RLHF, so the experimental domains focus on tasks where learning the utility function is more challenging than optimizing it. However, real-world RLHF systems often use large deep learning models to tackle challenging problems. Future work will scale insights gained from working with the HUB formalism to reward modeling for large language modeling and deep reinforcement learning systems.

References

[1] Alexander Pan, Kush Bhatia, and Jacob Steinhardt. The effects of reward misspecification: Mapping and mitigating misaligned models. *arXiv preprint arXiv:2201.03544*, 2022.

- [2] Joar Skalse, Nikolaus HR Howe, Dmitrii Krasheninnikov, and David Krueger. Defining and characterizing reward hacking. *arXiv preprint arXiv:2209.13085*, 2022.
- [3] Simon Zhuang and Dylan Hadfield-Menell. Consequences of misaligned AI. In *Advances in Neural Information Processing Systems*, pages 15763–15773, 2020.
- [4] Rachel Thomas and David Uminsky. The problem with metrics is a fundamental problem for AI. *arXiv preprint arXiv:2002.08512*, 2020.
- [5] Victoria Krakovna, Jonathan Uesato, Vladimir Mikulik, Matthew Rahtz, Tom Everitt, Ramana Kumar, Zac Kenton, Jan Leike, and Shane Legg. Specification gaming: the flip side of AI ingenuity. *DeepMind Blog*, 2020.
- [6] Paul Christiano, Jan Leike, Tom B Brown, Miljan Martic, Shane Legg, and Dario Amodei. Deep reinforcement learning from human preferences. *Advances in Neural Information Processing Systems*, June 2017.
- [7] Kimin Lee, Laura Smith, and Pieter Abbeel. PEBBLE: Feedback-efficient interactive reinforcement learning via relabeling experience and unsupervised pre-training. *arXiv preprint arXiv:2106.05091*, June 2021.
- [8] Nisan Stiennon, Long Ouyang, Jeffrey Wu, Daniel Ziegler, Ryan Lowe, Chelsea Voss, Alec Radford, Dario Amodei, and Paul F Christiano. Learning to summarize with human feedback. *Advances in Neural Information Processing Systems*, 33:3008–3021, 2020.
- [9] OpenAI. GPT-4 technical report, 2023.
- [10] Anthropic. Introducing Claude, 2023. URL <https://www.anthropic.com/index/introducing-claude>.
- [11] Hugo Touvron, Louis Martin, Kevin Stone, Peter Albert, Amjad Almahairi, Yasmine Babaei, Nikolay Bashlykov, Soumya Batra, Prajjwal Bhargava, Shrutu Bhosale, Dan Bikel, Lukas Blecher, Cristian Canton Ferrer, Moya Chen, Guillem Cucurull, David Esiobu, Jude Fernandes, Jeremy Fu, Wenyin Fu, Brian Fuller, Cynthia Gao, Vedanuj Goswami, Naman Goyal, Anthony Hartshorn, Saghar Hosseini, Rui Hou, Hakan Inan, Marcin Kardas, Viktor Kerkez, Madian Khabsa, Isabel Kloumann, Artem Korenev, Punit Singh Koura, Marie-Anne Lachaux, Thibaut Lavril, Jenya Lee, Diana Liskovich, Yinghai Lu, Yuning Mao, Xavier Martinet, Todor Mihaylov, Pushkar Mishra, Igor Molybog, Yixin Nie, Andrew Poulton, Jeremy Reizenstein, Rashi Rungta, Kalyan Saladi, Alan Schelten, Ruan Silva, Eric Michael Smith, Ranjan Subramanian, Xiaoqing Ellen Tan, Binh Tang, Ross Taylor, Adina Williams, Jian Xiang Kuan, Puxin Xu, Zheng Yan, Iliyan Zarov, Yuchen Zhang, Angela Fan, Melanie Kambadur, Sharan Narang, Aurelien Rodriguez, Robert Stojnic, Sergey Edunov, and Thomas Scialom. Llama 2: Open foundation and fine-tuned chat models, 2023.
- [12] Google. Bard, 2023. URL <https://bard.google.com/>.
- [13] Yuntao Bai, Andy Jones, Kamal Ndousse, Amanda Askell, Anna Chen, Nova DasSarma, Dawn Drain, Stanislav Fort, Deep Ganguli, Tom Henighan, et al. Training a helpful and harmless assistant with reinforcement learning from human feedback. *arXiv preprint arXiv:2204.05862*, 2022.
- [14] Stephen Casper, Xander Davies, Claudia Shi, Thomas Krendl Gilbert, Jérémy Scheurer, Javier Rando, Rachel Freedman, Tomasz Korbak, David Lindner, Pedro Freire, Tony Wang, Samuel Marks, Charbel-Raphael Segerie, Micah Carroll, Andi Peng, Phillip Christoffersen, Mehul Damani, Stewart Slocum, Usman Anwar, Anand Siththaranjan, Max Nadeau, Eric J. Michaud, Jacob Pfau, Dmitrii Krasheninnikov, Xin Chen, Lauro Langosco, Peter Hase, Erdem Biyik, Anca Dragan, David Krueger, Dorsa Sadigh, and Dylan Hadfield-Menell. Open problems and fundamental limitations of reinforcement learning from human feedback. *arXiv preprint arXiv:2307.15217*, 2023.
- [15] Long Ouyang, Jeffrey Wu, Xu Jiang, Diogo Almeida, Carroll Wainwright, Pamela Mishkin, Chong Zhang, Sandhini Agarwal, Katarina Slama, Alex Ray, et al. Training language models to follow instructions with human feedback. *Advances in Neural Information Processing Systems*, 35:27730–27744, 2022.
- [16] Joey Hong, Kush Bhatia, and Anca Dragan. On the sensitivity of reward inference to misspecified human models. *arXiv preprint arXiv:2212.04717*, 2022.
- [17] Rachel Freedman, Rohin Shah, and Anca Dragan. Choice set misspecification in reward inference. *arXiv preprint arXiv:2101.07691*, 2021.
- [18] Joar Skalse and Alessandro Abate. Misspecification in inverse reinforcement learning. *arXiv preprint arXiv:2212.03201*, 2022.
- [19] Smitha Milli and Anca Dragan. Literal or pedagogic human? Analyzing human model misspecification in objective learning. *Uncertainty in Artificial Intelligence*, 2020.
- [20] Oliver Daniels-Koch and Rachel Freedman. The expertise problem: Learning from specialized feedback. In *NeurIPS Workshop on ML Safety*, November 2022.

- [21] Eric J Michaud, Adam Gleave, and Stuart Russell. Understanding learned reward functions. *arXiv preprint arXiv:2012.05862*, 2020.
- [22] Peter Barnett, Rachel Freedman, Justin Svegliato, and Stuart Russell. Active reward learning from multiple teachers. In *AAAI Workshop on Artificial Intelligence Safety*, 2023.
- [23] Michael L Littman, Anthony R Cassandra, and Leslie Pack Kaelbling. Learning policies for partially observable environments: Scaling up. In *Journal of Machine Learning Research*, pages 362–370. Elsevier, 1995.
- [24] David Silver and Joel Veness. Monte-Carlo planning in large POMDPs. *Advances in Neural Information Processing Systems*, 23, 2010.
- [25] Zachary Sunberg and Mykel Kochenderfer. Online algorithms for POMDPs with continuous state, action, and observation spaces. In *International Conference on Automated Planning and Scheduling*, volume 28, pages 259–263, 2018.
- [26] Justin Lo, Krutika Amin, Imani Telesford, Lindsey Dawson, and Jennifer Kates. Prices for COVID-19 testing, May 2023. URL <https://www.healthsystemtracker.org/brief/prices-for-covid-19-testing/>.
- [27] Jesús Rufino, Carlos Baquero, Davide Frey, Christin A Glorioso, Antonio Ortega, Nina Reščič, Julian Charles Roberts, Rosa E Lillo, Raquel Menezes, Jaya Prakash Champati, et al. Using survey data to estimate the impact of the omicron variant on vaccine efficacy against COVID-19 infection. *Scientific Reports*, 13(1):900, 2023.
- [28] Alexander Harmon, Celina Chang, Nol Salcedo, Brena Sena, Bobby Brooke Herrera, Irene Bosch, and Laura E Holberger. Validation of an at-home direct antigen rapid test for COVID-19. *JAMA Network Open*, 4(8): e2126931–e2126931, 2021.
- [29] Rachelle N Binny, Patricia Priest, Nigel P French, Matthew Parry, Audrey Lustig, Shaun C Hendy, Oliver J Maclaren, Kannan M Ridings, Nicholas Steyn, Giorgia Vattiato, et al. Sensitivity of reverse transcription polymerase chain reaction tests for severe acute respiratory syndrome coronavirus 2 through time. *The Journal of Infectious Diseases*, 227(1):9–17, 2023.
- [30] Herbert Robbins. Some aspects of the sequential design of experiments. *American Mathematical Society*, 58(5): 527–535, 1952.
- [31] Aleksandrs Slivkins. Introduction to multi-armed bandits. *Foundations and Trends in Machine Learning*, 12(1-2): 1–286, 2019.
- [32] Andrew Y Ng and Stuart Russell. Algorithms for inverse reinforcement learning. In *International Conference on Machine Learning*, volume 1, page 2, 2000.
- [33] Pieter Abbeel and Andrew Y Ng. Apprenticeship learning via inverse reinforcement learning. In *21st International Conference on Machine Learning*, page 1, 2004.
- [34] B D Ziebart. *Modeling Purposeful Adaptive Behavior with the Principle of Maximum Causal Entropy*. PhD thesis, Carnegie Mellon University, 2010.
- [35] Dylan Hadfield-Menell, Stuart J Russell, Pieter Abbeel, and Anca Dragan. Cooperative inverse reinforcement learning. *Advances in Neural Information Processing Systems*, 29, 2016.
- [36] Dhruv Malik, Malayandi Palaniappan, Jaime Fisac, Dylan Hadfield-Menell, Stuart Russell, and Anca Dragan. An efficient, generalized bellman update for cooperative inverse reinforcement learning. In *International Conference on Machine Learning*, pages 3394–3402. PMLR, 2018.
- [37] Daniel S Bernstein, Robert Givan, Neil Immerman, and Shlomo Zilberstein. The complexity of decentralized control of Markov decision processes. *Mathematics of Operations Research*, 27(4):819–840, 2002.
- [38] Rohin Shah, Pedro Freire, Neel Alex, Rachel Freedman, Dmitrii Krasheninnikov, Lawrence Chan, Michael D Dennis, Pieter Abbeel, Anca Dragan, and Stuart Russell. Benefits of assistance over reward learning. *NeurIPS Workshop on Cooperative AI*, 2020.

A Theorem 1 Proof

Theorem 1. *If the predicted utility function $\hat{\mathcal{U}}$ and the predicted arm distribution $\hat{\mathcal{D}}^{\mathcal{C}}$ are estimated by executing Algorithm 1 with T samples, then $\hat{\mathcal{U}} \rightarrow \mathcal{U}^*$ and $\hat{\mathcal{D}}^{\mathcal{C}} \rightarrow \mathcal{D}^{\mathcal{C}*}$ as $T \rightarrow \infty$.*

Proof (Sketch). Since the number of arms is finite and they are pulled uniformly as $T \rightarrow \infty$, the number of times that a given arm c^k is pulled approaches infinity. Since each pull samples an item from the true distribution \mathcal{D}^{k*} i.i.d., the empirical distribution $\hat{\mathcal{D}}^k$ will approach \mathcal{D}^{k*} in the limit of infinite pulls. This argument applies for all arms $c^k \in \mathcal{C}$, so $\hat{\mathcal{D}}^{\mathcal{C}} \rightarrow \mathcal{D}^{\mathcal{C}*}$ as $T \rightarrow \infty$. Similarly, in the limit of infinite queries, $\hat{P}(\beta, (i, j))$ will approach $P^*(\beta, (i, j)) = \Pr(i \succ j; \beta, \mathcal{U}^*)$, the true probability that teacher b prefers item i over item j , as determined by Equation 1. Given $\beta, (i, j)$ and $\hat{P}(\beta, (i, j))$ from the first T timesteps, we can calculate $\Delta_{ij} = \hat{\mathcal{U}}(i) - \hat{\mathcal{U}}(j)$ using Equation 2. Given $\Delta = [\Delta_{01}, \Delta_{02}, \dots, \Delta_{NN}]$, u_{max} and u_{min} , we can calculate $\hat{\mathcal{U}}$ as described in Algorithm 1. $\hat{\mathcal{U}} \rightarrow \mathcal{U}^*$ as $\hat{P} \rightarrow P^*$, which occurs as $T \rightarrow \infty$. \square

B Theorem 2 Proof

Theorem 2. *Given two items $i, j \in \mathcal{I}$ where $\mathcal{U}(i) < \mathcal{U}(j)$, the preference probability $P = \Pr(i \succ j; \beta_m, \mathcal{U})$ from Equation 1, and the scaling factor $a = -\Delta_{ij}^{-1}$, we can calculate β_m as follows:*

$$\beta_m = a \cdot \ln\left(\frac{1}{P} - 1\right). \quad (4)$$

Proof (Sketch). First, we define an affine mapping function $f_{a,b}(x) = ax + b$ such that $f_{a,b}(\mathcal{U}(i)) = 0$ and $f_{a,b}(\mathcal{U}(j)) = 1$. Lemma 3 shows that this is always possible when $\mathcal{U}(i) \neq \mathcal{U}(j)$. Let a, b be the parameters that make this mapping for these particular values of $\mathcal{U}(i)$ and $\mathcal{U}(j)$.

Next, suppose we have that $\beta'_m = \frac{1}{a}\beta_m$, it follows that:

$$\begin{aligned} P &= \Pr(i^0 \succ i^1; \beta_m, \mathcal{U}) \\ &= \frac{\exp(\beta_m \mathcal{U}(i))}{\exp(\beta_m \mathcal{U}(i)) + \exp(\beta_m \mathcal{U}(j))} && \text{(by Equation 1)} \\ &= \frac{\exp\left(\frac{\beta_m}{a} \cdot a\mathcal{U}(i) + \frac{\beta_m}{a} b\right)}{\exp\left(\frac{\beta_m}{a} \cdot a\mathcal{U}(i) + \frac{\beta_m}{a} b\right) + \exp\left(\frac{\beta_m}{a} \cdot a\mathcal{U}(j) + \frac{\beta_m}{a} b\right)} \\ &= \frac{\exp(\beta'_m \cdot (a\mathcal{U}(i) + b))}{\exp(\beta'_m \cdot (a\mathcal{U}(i) + b)) + \exp(\beta'_m \cdot (a\mathcal{U}(j) + b))} && \text{(by definition of } \beta'_m) \\ &= \frac{\exp(\beta'_m \cdot f_{a,b}(\mathcal{U}(i)))}{\exp(\beta'_m \cdot f_{a,b}(\mathcal{U}(i))) + \exp(\beta'_m \cdot f_{a,b}(\mathcal{U}(j)))} && \text{(by definition of } f_{a,b}) \\ &= \frac{\exp(0)}{\exp(0) + \exp(\beta'_m)} = \frac{1}{1 + \exp(\beta'_m)}. \end{aligned}$$

Finally, solving for β'_m yields $\beta'_m = \frac{1}{a}\beta_m = \ln\left(\frac{1}{P} - 1\right) \rightarrow \beta_m = a \cdot \ln\left(\frac{1}{P} - 1\right)$. \square

Lemma 3. *Given any two numbers $m, n \in \mathbb{R}$ such that $m \neq n$, there exists an affine transformation $f_{a,b} : \mathbb{R} \rightarrow \mathbb{R}$ that maps the greater number to 1 and the lesser number to 0.*

Proof (Sketch). Suppose that $m > n$ without loss of generality. We therefore must solve the following system of equations: $f_{a,b}(m) = am + b = 1$ and $f_{a,b}(n) = an + b = 0$. The solution is $a = \frac{-1}{n-m}$ and $b = \frac{m}{n-m} + 1$, which always exists when $m \neq n$. \square

C POMCPOW Rollout Policies

ATS solves the HUB-POMDP using *partially observable Monte-Carlo planning with observation widening* (POMCPOW) augmented with a custom rollout policy for estimating the value of leaf nodes in the search tree. We evaluate a *random action* rollout policy, which takes actions uniformly at random from $\mathcal{A} = \mathcal{C} \cup \beta$, a *random arm* rollout policy,

which chooses arms uniformly at random from \mathcal{C} , and a *best arm* policy, which calculates which arm has the highest expected utility *according to the current belief b* , then always chooses that arm.

Since a utility-maximizing agent will choose arms more often if it believes them to have higher utility, the *best arm* policy rollouts most closely resemble the actions the actual policy would take from belief b , yielding the most accurate value estimates. As a result, ATS with best arm rollouts outperforms the alternatives on the paper recommender domain, as shown in Figure 9. Results are averaged across 25 runs on 20 different paper recommendation tasks.

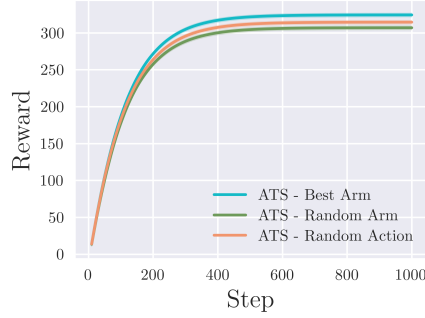


Figure 9: Performance of ATS with various rollout policies. The best arm rollout policy outperforms the random arm and random action rollout policies. All data is averaged across 25 runs on each of 20 HUB problems, smoothed over 10 steps, and discounted with $\gamma = 0.99$.

D HUB Cost effects

We investigate the impacts of teacher query cost on ATS performance by varying professor feedback costs in the paper recommendation domain. We set linear costs $F = \{-1, -2, -3\}$ and scale them by a *cost multiplier*. As in the other paper recommendation experiments, results are averaged across 25 runs on 20 different paper recommendation tasks.

We find that ATS responds rationally to changes in costs, querying teachers more sparingly (Figure 10b) and consequently identifying the best arm more slowly (Figure 10a as overall costs increase. This leads to a slight decrease in overall performance (Figure 10c).

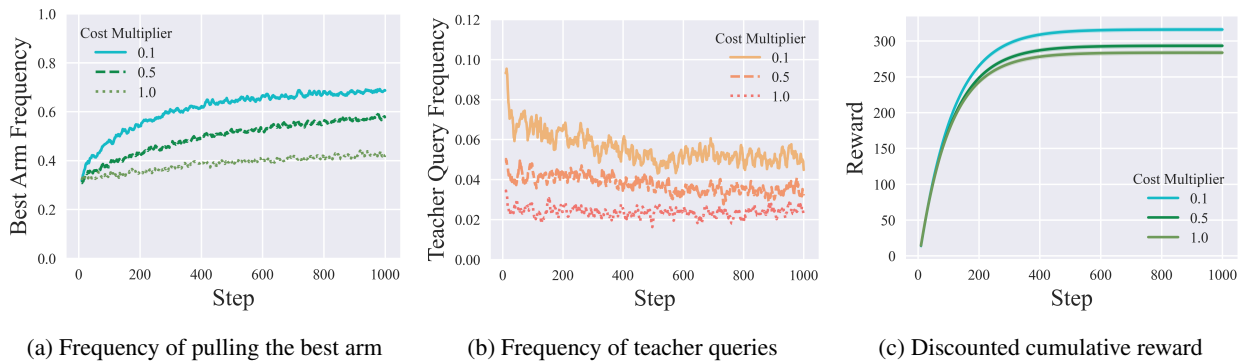


Figure 10: ATS behavior and performance varies with teacher query costs. Data is averaged across 25 runs on 20 paper recommendation HUB problems and smoothed over 10 steps.